

# Anomalous Preservation of Pure Methane Hydrate at 1 atm

Laura A. Stern,\* Susan Circone,<sup>†</sup> and Stephen H. Kirby<sup>‡</sup>

U.S. Geological Survey, 345 Middlefield Rd, MS/977, Menlo Park, California 94025

William B. Durham<sup>§</sup>

U.C. Lawrence Livermore National Laboratory, Livermore, California 94550

Received: August 23, 2000; In Final Form: December 7, 2000

Direct measurement of decomposition rates of pure, polycrystalline methane hydrate reveals a thermal regime where methane hydrate metastably “preserves” in bulk by as much as 75 K above its nominal equilibrium temperature (193 K at 1 atm). Rapid release of the sample pore pressure at isothermal conditions between 242 and 271 K preserves up to 93% of the hydrate for at least 24 h, reflecting the greatly suppressed rates of dissociation that characterize this regime. Subsequent warming through the H<sub>2</sub>O ice point then induces rapid and complete dissociation, allowing controlled recovery of the total expected gas yield. This behavior is in marked contrast to that exhibited by methane hydrate at both colder (193–240 K) and warmer (272–290 K) test conditions, where dissociation rates increase monotonically with increasing temperature. Anomalous preservation has potential application for successful retrieval of natural gas hydrate or hydrate-bearing sediments from remote settings, as well as for temporary low-pressure transport and storage of natural gas.

## Introduction

Methane hydrate, CH<sub>4</sub>·*n*H<sub>2</sub>O, where *n* ≥ 5.75, is a nonstoichiometric compound consisting of an open network of H<sub>2</sub>O molecules that are hydrogen-bonded in a manner similar to ice and interstitially encaging CH<sub>4</sub> gas molecules. This icy substance has generated considerable recent interest as a globally distributed mineral that harbors a significant yet virtually untapped hydrocarbon source,<sup>1,2</sup> as an icy compound in outer solar system environments,<sup>3</sup> and as a manufactured material that is a potential medium for safe storage and transport of natural gas.<sup>2,4</sup> Hydrates in sediments on continental margins may also impact global climate and seafloor mechanical stability, due to the sensitivity of their stability to climate-induced changes in sea level and seabottom temperatures.<sup>5–9</sup> In spite of this interest, there remains a surprising lack of reliable experimental measurements on many of the fundamental physical properties of pure methane hydrate, as well as on those of many other end-member hydrocarbon hydrates. Compounding this problem is the difficulty in retrieving pristine samples of naturally occurring gas hydrate on which to make such measurements.

Here we report on some unexpected results of controlled decomposition and phase stability experiments conducted at 1 atm on pure, polycrystalline methane hydrate, over the temperature range 193–290 K, as it dissociates to CH<sub>4</sub> (gas) + H<sub>2</sub>O (solid or liquid). These results demonstrate an unusual dependency of methane hydrate stability on its pressure–temperature–time (*P–T–t*) path prior to and during dissociation. Of particular note is a warm-temperature regime in which dissociation rates are highly suppressed, enabling preservation of bulk quantities of methane hydrate for extended duration with minimal dis-

sociation. Such anomalous behavior may have important application to strategies used for retrieval of remote natural gas hydrates or hydrate-bearing sediments by drill core, as well as for gas production rates from natural hydrocarbon hydrate when using depressurization methods to decompose the hydrate.

## Experimental Section

**Sample Preparation.** Cylindrical test specimens of methane hydrate were grown under static conditions by combining cold, pressurized CH<sub>4</sub> gas (250 K, 27 MPa) with granular H<sub>2</sub>O ice “seeds” (180–250 μm grain size) in stainless steel reaction vessels.<sup>10,11</sup> Heating the reactants above the H<sub>2</sub>O ice melting point promotes the general reaction CH<sub>4</sub> (g) + 5.9H<sub>2</sub>O (s→l) → CH<sub>4</sub>·5.9H<sub>2</sub>O (methane hydrate), where slow melting of the water ice facilitates the hydrate-forming reaction.<sup>10–12</sup> Complete reaction was achieved by continued warming to 290 K and ~30 MPa for approximately 12–15 h (Figure 1A). Sample temperature (*T*<sub>sample</sub>) was monitored by four axially positioned thermocouples (see inset in Figure 2B), and methane gas pressure (*P*) was monitored by a Heise bourdon gauge and pressure transducers. The reaction vessels were immersed in a 12 L ethanol bath and warmed by a temperature-controlled ring immersion heater. Calibrated probes (RTDs) monitored the bath temperature, also referred to here as the external test temperature (*T*<sub>ext</sub>). Full reaction was determined from the *P–T*<sub>sample</sub> synthesis record, as hydrate formation consumes a known mass of the vapor phase, causing a predictable pressure offset in the *P–T* record.<sup>10,11</sup> Final hydrate samples are 2.54 cm in diameter by about 9.3 cm in length, and typically contain 30 g of hydrate with 29 ± 1% porosity. The product is highly reproducible in composition as well as in grain and pore characteristics: samples are pure, cohesive, polycrystalline methane hydrate of composition CH<sub>4</sub>·5.89H<sub>2</sub>O (±0.01 H<sub>2</sub>O), and have controlled grain size (250–300 μm) with random crystallographic orientation and no detectable secondary phases.<sup>13</sup>

\* Corresponding author. Tel: (650) 329-4811. Fax: (650) 329-5163. E-mail: lsstern@usgs.gov.

<sup>†</sup> Tel: (650) 329-5674. Fax: (650) 329-5163. E-mail: scircone@usgs.gov.

<sup>‡</sup> Tel: (650) 329-4847. Fax: (650) 329-5163. E-mail: skirby@usgs.gov.

<sup>§</sup> Tel: (925) 422-7046. Fax: (925) 423-1057. E-mail: durham1@llnl.gov.

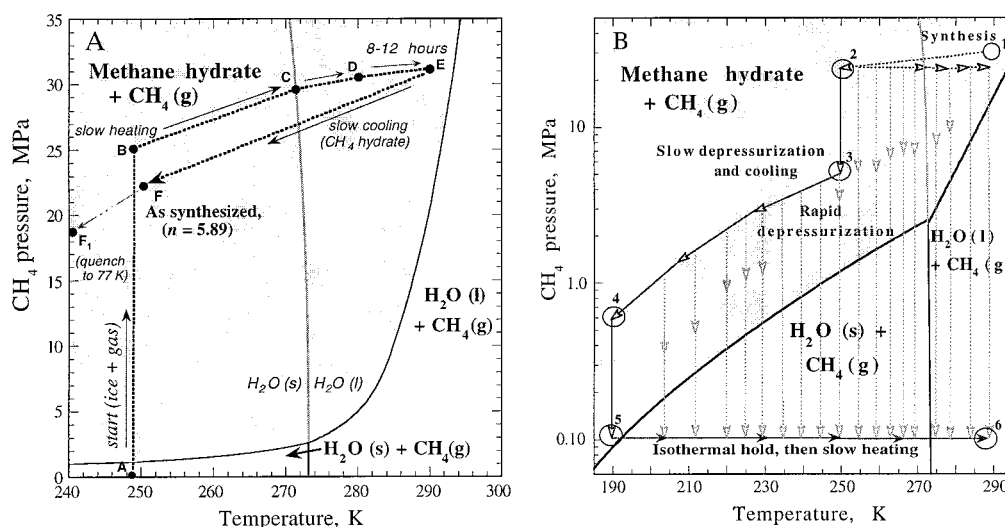


**Figure 1.** Experimental conditions for methane hydrate synthesis (A) and dissociation (B) in relation to the  $\text{CH}_4$ – $\text{H}_2\text{O}$  phase diagram. Phase equilibria data are from ref 2. Shaded regions show methane hydrate stability field. The melting curve of  $\text{H}_2\text{O}$  is designated by the solid gray curve. Solid, liquid, and gas phases are denoted s, l, and g, respectively. (A) Black dotted lines connecting points A–F trace the  $P$ – $T$  reaction path during methane hydrate synthesis from ice + gas mixtures.  $\text{H}_2\text{O}$  “seed” ice at 250 K (point A) is first pressurized with  $\text{CH}_4$  gas to 25 MPa (point B). Heating these reactants under static conditions through the  $\text{H}_2\text{O}$  melting point (C) and up to 290 K (C–D–E) with subsequent isothermal hold for 8–12 h (E) promotes full and efficient conversion of the ice to gas hydrate. Samples are then cooled to 250 K (F) and either dissociated in situ by the procedures detailed below, or quenched ( $F_1$ ) and removed from the apparatus. The “ $n$ ” number represents the stoichiometry of the final “as-synthesized” product. (B)  $P$ – $T$  paths for destabilizing as-synthesized methane hydrate to  $\text{CH}_4$  (gas) +  $\text{H}_2\text{O}$  (ice or water) for measurement of dissociation rates, stoichiometry, and stability behavior. (1) The “temperature ramping” method, in which samples, following synthesis (point 1) are slowly cooled and depressurized to  $T < 193$  K and  $P = 0.1$  MPa (points 2–5), then slowly heated above the dissociation curve at a rate of  $\sim 10$  K/h (points 5–6). (2) The “rapid depressurization” method in which samples are first depressurized to a smaller overstep of the equilibrium curve at a chosen isothermal test temperature ( $T_{\text{ext}}$ ), then quickly depressurized to 0.1 MPa to immediately destabilize the hydrate. After dissociation proceeds at  $T_{\text{ext}}$  for some time interval ( $< 1$  h to several days) such that dissociation either reaches a steady state rate or ceases, the sample is warmed slowly through the ice point to ensure full decomposition of residual hydrate and/or release of gas trapped within ice grains or along grain boundaries.

**Gas Flow Rate and Mass Measurement.** Hydrate dissociation rates and stoichiometry were measured by monitoring the flow of methane as it evolved from a destabilized sample, using a custom-built gas flow meter and collection instrument connected directly to the reaction vessel.<sup>14</sup> The direct nature of these measurements avoids the structural, compositional, and reproducibility problems inherent to sample handling and transfer procedures at ambient pressure, or exposure of test material to liquid nitrogen or cold air. The flow meter operates on the principles of a Torricelli tube and measures the volume (and hence mass) of gas evolved from a dissociating sample as well as precisely measuring the rate of gas evolution.<sup>14,15</sup>

**Dissociation Procedures.** Either of two general procedures were followed to take samples from postsynthesis conditions of elevated pressure down to 0.1 MPa prior to dissociation. The first of these, “temperature ramping”, involves initial slow cooling and depressurization of the sample, remaining just within the methane hydrate stability field (Figure 1B, solid lines). When the sample has cooled below 193 K,  $P$  is lowered to 0.1 MPa and the sample is opened to the flow meter. Warming the sample above the methane hydrate dissociation temperature (193 K at 0.1 MPa) by heating the surrounding fluid bath then destabilizes the hydrate, and the evolved gas is collected in the flow meter.<sup>14</sup> Further warming through the melting point of ice (273.15 K) is then required to fully melt the ice product and release any remaining gas. The temperature-ramping method permits sample stabilization at  $T < 193$  K and  $P = 0.1$  MPa for an extended time prior to dissociation, and thus allows release of any trapped pore-space gas or adsorbed methane from the sample (easily detectable by baseline shifts recorded by the flow meter); it is therefore an ideal method for precise measurement of sample stoichiometry.<sup>13,16</sup> Such measurements are needed to complement the pressure-release dissociation tests discussed below,

both for the characterization of our synthetic hydrate and for accurate prediction of the expected gas yield from pressure-release tests.

The second dissociation method, termed “rapid depressurization” or “pressure release” (Figure 1B, dashed lines), involves slowly depressurizing the sample to several MPa above the equilibrium curve, allowing the sample to reequilibrate with the external fluid bath temperature ( $T_{\text{ext}}$ ), then rapidly venting the remaining gas pressure on the sample to 0.1 MPa over a 6–12 s interval.<sup>17</sup> The vent is then quickly closed while simultaneously opening the sample to the flow meter, allowing collection and flow measurement of the hydrate-forming gas. For samples tested by rapid depressurization at  $T < 273$  K, it is necessary to then warm them through 273 K after completion of the isothermal portion of main dissociation event as in the ramping tests discussed above, to ensure release of all methane gas from the sample. The pressure-release method is used to quickly access a thermal region where hydrate should actively dissociate at 0.1 MPa, and thus allows mapping of dissociation behavior as a function of isothermal (external) test temperature, including the  $P$ – $T$  region where hydrate is predicted to dissociate to liquid water + gas.<sup>15</sup> Several additional samples in this study were taken through a combination of both the pressure-release and temperature-ramping procedures, and are discussed separately below.

## Results and Discussion

**Systematics of Methane Hydrate Dissociation.** Methane hydrate dissociation behavior was found to vary considerably depending on the particular pressure–temperature–time ( $P$ – $T$ – $t$ ) path used to destabilize the hydrate. Samples decomposed by temperature-ramping procedures exhibited highly reproducible decomposition behavior in which approximately

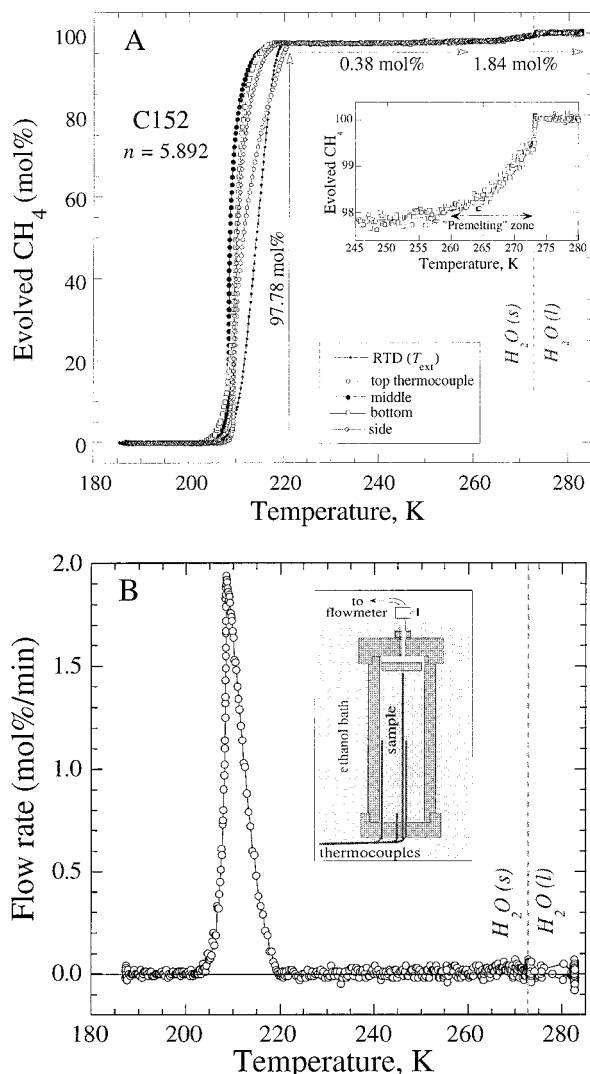


**Figure 2.** A typical dissociation profile (A) and flow-rate profile (B) for a sample of methane hydrate grown from 26 g of  $\text{H}_2\text{O}$  ice and dissociated in situ by temperature-ramping procedures (Figure 1B). Symbols correspond to top, middle, bottom, and side thermocouple positioning as shown in inset of (B). Samples tested in this manner yield  $0.244 (\pm 0.001)$  moles of  $\text{CH}_4$  gas, corresponding to a stoichiometry of  $\text{CH}_4 \cdot 5.89\text{H}_2\text{O}$  ( $\pm 0.01\text{H}_2\text{O}$ ), and defining the total expected gas for the pressure-release tests shown in Figures 3 and 4. Most gas evolves over the  $T$  range 200–220 K (A), with the highest flow rate typically measured at  $209 \pm 1$  K (B). During moderate to rapid dissociation, sample thermocouples systematically lag the external bath temperature ( $T_{\text{ext}}$ ) due to the endothermic reaction. Samples then release little gas (0.3–0.8 mol %) upon further heating from 220 to 260 K. The remaining gas is slowly but progressively released when warmed into the “premelting”<sup>29</sup> zone of ice at  $T > 260$  K (expanded in inset). The final percentage of gas is quickly released at 273.1 K, presumably as the accumulating ice product melts and releases the residual trapped hydrate or gas from within it.

97% of the expected amount of gas evolved over the temperature range  $198 \text{ K} < T_{\text{sample}} < 220 \text{ K}$  (Figure 2A), attaining a maximum flow rate near 209 K (Figure 2B). Upon further heating to 260 K, samples release little gas ( $< 1\%$ ; Figure 2A). Above 260 K, degassing resumes slowly but progressively until  $T$  reaches 273 K, at which point a small pulse of gas evolves that typically accounts for the remaining 2% of the total yield (see Figure 2A, inset).

In a manner consistent with the temperature-ramping tests, methane hydrate samples that were destabilized by pressure-release methods over the range  $195 \text{ K} \leq T_{\text{ext}} \leq 240 \text{ K}$  exhibited

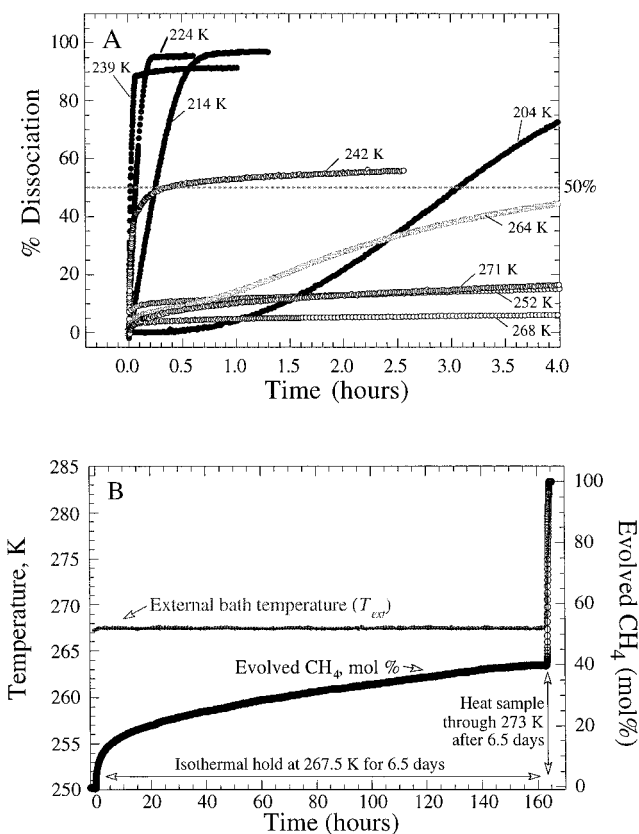


**Figure 3.** Representative curves from rapid depressurization tests, showing the unusual rate effect of temperature on hydrate dissociation to ice + gas at 1 atm. (A) Dissociation rates of samples tested over the temperature range 204–270 K. Up to 240 K (solid symbol curves), methane hydrate dissociates at continuously increasing rates with increasing  $T_{\text{ext}}$ . Only the isothermal portion of the experiments are shown here; heating through 273 K then releases all remaining gas, usually totaling within 3% of the expected amount (see text and ref 18). From 242 to 271 K, however, dissociation rates become highly suppressed (open symbol curves), resulting in large fractions of the hydrate “preserving” in many tests for at least many days. Dissociation rates in this regime are less suppressed over the range 256–264 K than at temperatures 5 K colder or warmer. (B) Profile of a rapid depressurization test at 267.5 K (74 K above the equilibrium dissociation temperature), showing survival of 60% of the hydrate after 6 days. The remaining gas yield was then recovered by heating the sample through 273 K, as shown at right.

monotonic dissociation behavior with rates increasing with test temperature (Figures 3A and 4), as would be expected with the increasing thermal overstep of the stability field. Samples tested at 204 K dissociated over approximately 5 h, while those tested at 239 K dissociated within 7 min (Figure 3A, solid-symbol curves), where times correspond to the duration of the main dissociation event, or about 88% reaction. The remaining gas in these tests was released when later warmed through 273 K.<sup>18</sup> A significant thermal lag between  $T_{\text{sample}}$  and  $T_{\text{ext}}$  due to the heat absorption caused by the endothermic dissociation reaction was also measured throughout the main dissociation phase of these tests. As expected, more rapid dissociation promoted greater thermal variance between  $T_{\text{sample}}$  and  $T_{\text{ext}}$ , ranging from a 0.4 K difference during the main dissociation event at  $T_{\text{ext}} = 204 \text{ K}$ , to nearly a 30 K difference at  $T_{\text{ext}} = 240 \text{ K}$ . These results are consistent with temperature-ramping tests, which indicated a sharp decrease in dissociation rates at temperatures below 208–210 K (Figure 2B).

**Anomalous Preservation Regime.** Samples that were rapidly depressurized at isothermal test conditions ranging from



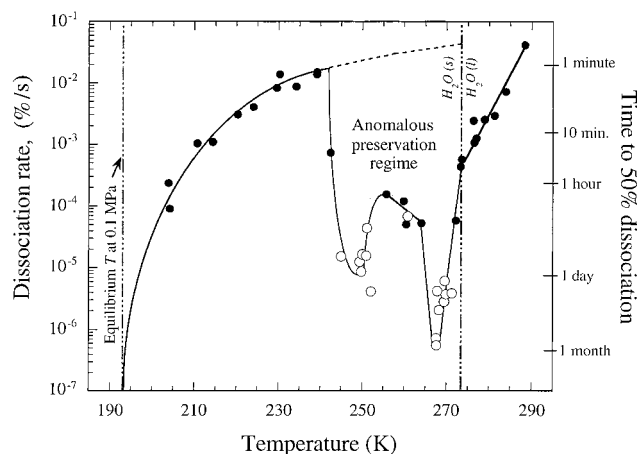


**Figure 4.** Average rates at which methane hydrate samples reach 50% dissociation at 0.1 MPa, following destabilization at constant (external) test temperatures by the pressure-release method discussed in the text and shown in Figure 1B. Dissociation rates vary considerably over the course of each experiment (see Figure 3A), and the rates plotted here are the inverse of the total time required for each sample to attain 50% dissociation (see also time scale on right). The equilibrium dissociation temperature for methane hydrate at 0.1 MPa is indicated at 193 K, and the  $H_2O$  melting temperature is shown at 273.1 K. Above 193 K, hydrate dissociation rates increase monotonically with increasing test temperatures over the ranges 193–240 K and 271–290 K. The “anomalous preservation” thermal regime at 242–271 K, however, is characterized by markedly depressed dissociation rates that are orders of magnitude slower than those predicted by extrapolation of the lower temperature tests (dashed curve). Rates are less suppressed between 255 and 264 K than at those temperatures slightly colder (248–254 K) or warmer (265–271 K). Open symbols represent extrapolated rates for those runs that preserved so successfully that they never attained 50% dissociation over the isothermal portion of the tests. Extrapolated rates for these tests are conservative (see text), and the actual rates are most likely considerably slower than shown here.

$242 \leq T_{\text{ext}} \leq 271$  K displayed dissociation behavior that diverged markedly from the monotonic behavior observed in all pressure-release tests conducted at temperatures both above and below this regime (Figures 3 and 4). Following the pressure-release treatment at  $242 \leq T_{\text{ext}} \leq 271$  K, samples displayed a brief-but-rapid dissociation phase in which they typically lost 5–20 vol % of their total expected gas yield (as defined in Figure 2A) within several seconds to tens of seconds of the pressure drop. During this initial degassing event,  $T_{\text{sample}}$  typically dropped by 3–7 K relative to  $T_{\text{ext}}$  due to adiabatic cooling of the methane as well as to heat absorption during dissociation. After this initial event, dissociation abruptly slowed to extremely low rates (typically  $<0.05\%/min$ ), and  $T_{\text{sample}}$  correspondingly rebounded to  $T_{\text{ext}}$ . The bulk of the sample then remained metastably “preserved” for extended duration. This preservation effect was most successful at  $T_{\text{ext}}$  at or just below 270 K, where large volume fractions of the hydrate (up to 93 vol %) survived for at least the 24 h of the isothermal hold portion of the experiment (Figure 3A, lower curves). In one test in which a sample initially lost approximately 16 vol % of its total yield after depressurization at 268 K, the sample was then held isothermal for over 6 days during which it continued to evolve approximately 4 vol % of its remaining gas yield per day (Figure 3B). The sample was then heated through 273 K, and the expected remainder of gas evolved quickly from the sample (Figure 3B, at right).

While some variation occurs on a sample-to-sample basis, the general expression of dissociation exhibited by virtually all samples subjected to rapid depressurization was very reproducible. Figure 4 maps the average rate that pressure-released

samples dissociated 50% of their full gas yield under isothermal test conditions, illustrating the thermal regions of monotonic vs anomalous behavior. As dissociation rates vary considerably during the course of each experiment (as shown in Figure 3A), the average rates plotted in Figure 4 represent the inverse of the time required for samples to evolve 50% of their gas yield (see also general time scale on Figure 4, at right). Many tests conducted between 245 and 272 K never attained 50% dissociation, due to the extraordinarily slow dissociation rates in portions of the anomalous preservation regime (Figure 4, open symbols). The times and average rates to 50% dissociation for these tests were extrapolated based on the rate of reaction measured near the end of the isothermal portion of the experiment; these extrapolations are therefore conservative estimates, as the rate of dissociation continuously decreases over time as the amount of remaining hydrate decreases.

Figure 4 also illustrates additional details within the anomalous preservation regime. While dissociation rates are highly reduced throughout this region, remaining orders of magnitude slower than those predicted by extrapolation of lower-temperature rates (compare open circles to dashed curve in Figure 4), all tests performed at 256–264 K displayed rates that were measurably higher than those at either 245–255 K or 265–271 K (Figures 3A and 4). The cause of this variation within the preservation regime is currently not known, but all tests conducted in this region confirmed its reproducibility.

The transition in dissociation rates from the low-temperature regime of continuous and monotonic dissociation to the anomalous preservation regime, as well as the transition from the preservation regime to the high-temperature regime at  $T_{\text{ext}} > 271$  K, are both sharply defined and well resolved experimentally (Figure 4). The transition from low-temperature behavior (195–240 K) to the preservation regime was observed in a series of twelve tests conducted over the interval 239–251 K, defining the onset of sample preservation with increasing  $T_{\text{ext}}$ . Similarly, above the upper limit of the preservation regime ( $>271$  K), 13 tests defined the manner by which dissociation behavior resumes more predictably, with increasing rates accompanying increasing temperatures (Figure 4; see also Figure 3 in ref 15). These tests also indicate that dissociation rates increase considerably more rapidly over the narrow thermal range 271–273 K than above 273 K where methane hydrate is predicted to dissociate to liquid water +  $CH_4$  gas (Figure 4). This may be related to a temperature buffering effect observed in all samples tested at  $T_{\text{ext}} > 273$  K; in 10 experiments conducted between 273 and 290 K,  $T_{\text{sample}}$  plummeted and buffered at 272.5 K for the duration of the main dissociation event, and the rates at which these samples dissociated were shown to be governed primarily by the rate of heat flow into them.<sup>15</sup>

One pressure-release test at 267.5 K was also conducted on a 30 g sample of pure, laboratory-synthesized  $CO_2$  hydrate. This sample likewise “preserved” in the manner displayed by pure methane hydrate tested at that temperature, indicating that warm-temperature preservation induced through rapid depressurization is not singular to the  $CH_4$ – $H_2O$  system.

**Physical Chemistry Considerations.** The physical chemistry of anomalous preservation remains enigmatic. Several samples of methane hydrate were first rapidly depressurized and stabilized at 250–270 K for at least 90 min, then cooled at varying rates (from several minutes to several hours) to 190 K. None exhibited any significant increase in dissociation rate during cooling. Two additional preserved samples were quenched to 77 K in liquid nitrogen and analyzed by X-ray diffraction,

verifying that the quenched material was structure I methane hydrate with very little ice in the sample interior.<sup>19</sup> Upon rewarming both the slowly cooled and the quenched material above 193 K, however, the bulk of the hydrate dissociated over the interval 198–218 K as observed in temperature-ramping tests discussed earlier. These results suggest that methane hydrate subjected to  $P$ – $T$ – $t$  conditions that place it within the anomalous preservation regime behaves effectively as if it were a different material or in a different geochemical state,<sup>20</sup> as opposed to the interpretation that anomalous preservation is maintained by an ongoing process or reaction. The exceedingly long duration of preservation observed in many of the tests further supports this interpretation; it was impractical to even roughly determine the full duration of optimal preservation, due to the extraordinarily suppressed dissociation rates combined with apparatus time constraints. However, if anomalous preservation converts ordinary methane hydrate to a structure with different intrinsic properties, significant cooling changes it back, as indicated by the behavior of preserved material following cooling and subsequent re-warming, and X-ray analyses of quenched samples.

Visual inspection and handling of preserved and quenched methane hydrate indicates that the material also undergoes textural changes. Quenched, preserved methane hydrate is significantly more competent and less prone to fracturing or flaking during cleaving and/or handling procedures than as-synthesized methane hydrate, and is noticeably less granular in appearance. To further investigate the effect of porosity, sample texture, and grain boundary effects on anomalous preservation, five additional pressure-release tests were conducted at 267–270 K on more porous methane hydrate and on a variety of hydrate + sediment mixtures.<sup>21</sup> These samples all exhibited rates of dissociation that were highly reduced relative to the extrapolated rates from the low- $T$  tests (Figure 4, dashed curve), but measurably faster than those measured on pure or more compact samples of methane hydrate. The textural observations, the lack of appreciable ice within the preserved material, and the results of tests on unconsolidated methane hydrate (and the one test on CO<sub>2</sub> hydrate) thus indicate that while the warm-temperature preservation effect is enhanced by hydrate-to-hydrate grain boundary contacts, it appears to be a structural or intrinsic material property of gas hydrate. Further investigation of the physical chemistry of the preservation effect by microscopy or spectroscopic techniques remains a challenge, however, due to the thermal irreversibility discussed above, requiring in situ analysis on rapidly depressurized material at warm-temperature isothermal conditions rather than on quenched material.

**Comparison to Other Reportings of Preservation.** Other occurrences of incomplete dissociation of gas hydrate below the ice point have been described in various hydrate systems, including synthetic methane hydrate,<sup>22–24</sup> deuteriohydrate of methane,<sup>25</sup> krypton hydrate,<sup>26</sup> and synthetic structure II hydrates,<sup>22,23,27</sup> as well as on recovered samples of various natural gas hydrates.<sup>25,28</sup> The “self” preservation effect described by Yakushev and Istomin on synthetic methane hydrate,<sup>22</sup> in which several samples were preserved in bulk for extended time, appears to be most similar to our own observations. It is difficult to compare quantitatively our investigation and mapping of the anomalous preservation regime with the results of others, however, due to insufficient information regarding the structure,  $P$ – $T$ – $t$  history, extent of “preservation”, or original hydrate composition in the material reported in these previous studies. These uncertainties are commonly due to either the presence of ice as a secondary phase, or in the case of recovered natural

gas hydrate, due to the unknown extent of decomposition and alteration during retrieval, transport, and handling processes. We also note that many structure II gas hydrates are stable to significantly warmer temperatures at ambient pressure than pure methane hydrate, and the extent and/or mechanisms of preservation may differ considerably for different compositions or structures of gas hydrate. Common to all the cases cited above, however, is that all the residual hydrate-forming gas is rapidly released upon heating the final material through the ice point.

In the previously reported cases of incomplete dissociation of gas hydrate at temperatures below the ice point, the formation of thin films of ice on the surface of decomposing hydrate,<sup>22</sup> or the presence of significant amounts of ice in the samples,<sup>23,25,26</sup> has commonly been invoked as a mechanism for explaining the preservation behavior. Davidson et al.,<sup>25</sup> for instance, speculated that ice produced by partial hydrate decomposition forms an impermeable coating on the remaining hydrate, and hence maintains an elevated internal methane pressure at or near the equilibrium pressure. Similarly, in the two-stage dissociation process observed by Handa on large crystals of krypton hydrate,<sup>25</sup> dissociation was speculated to start at the surface of the crystal, coating the hydrate with a layer of ice that effectively sealed the crystals and preventing further dissociation until the ice began to melt.

In dissociation tests conducted by the temperature-ramping method, we expect that the delayed release of the residual 2–5% gas represents small amounts of hydrate or gas becoming trapped within ice grain interiors or along ice grain boundaries as decomposition proceeds on a granular scale from surface to core, such that the remaining gas is subsequently released during “premelting”<sup>29</sup> and melting of the encapsulating ice (Figure 2A, inset). Consequently, the large amount of ice product in these samples may effectively “preserve” small amounts of hydrate up to 273 K by creating a thick mechanical barrier or seal around the hydrate, in a manner like that suggested by Davidson et al. or Handa.<sup>23,25,26</sup> Similarly, in recovered natural gas hydrates from remote, ocean-floor environments, ice mantles or rinds may encapsulate decomposing hydrate, such that at least small fractions of hydrate can be recovered after a lengthy retrieval process.

We remain skeptical, however, that such a shielding effect of ice could be the principal preservation mechanism for the anomalous preservation regime. In several tests conducted at 269–270 K, over 90% of the hydrate persisted for over 20 h (and until heated through the ice point) due to exceptionally low dissociation rates; if dissociation proceeds on a grain scale, this small amount of ice developing as a mantle on slowly dissociating grains of methane hydrate would provide a mantle thickness of approximately 4  $\mu\text{m}$  on each hydrate grain or grain cluster (typically  $\sim 250 \mu\text{m}$ ). Not only is it highly unlikely that such a thin skin of ice could sustain an internal methane pressure of approximately 2 MPa at 270 K and thereby “preserve” or shield the hydrate, but X-ray analyses suggests that the ice fraction does not occur uniformly throughout the samples on grain surfaces.<sup>19</sup> Furthermore, it is difficult to conceptualize how such shielding could effectively preserve rapidly depressurized methane hydrate in an irreversible manner, allowing preservation during slow cooling from 270 to 190 K, but not upon immediate rewarming of the same material above 193 K. We also note that the most optimal thermal region for preservation ( $269 \pm 1$  K) is well within the premelting zone of H<sub>2</sub>O ice, where increased dissociation rates are measured in the temperature-ramping tests (Figure 2A, inset). However, as warming of the preserved material through the melting point of ice induces rapid

dissociation and release of all the remaining gas, the presence of even small amounts of ice, or the mobility of molecular water at these temperatures, is somehow integral to the preservation effect.

## Summary

While the physical chemistry of the preservation behavior of methane hydrate remains elusive, the phenomenon is highly reproducible and is now well-defined. We provide here for the first time a detailed map of methane hydrate dissociation rates at 0.1 MPa of methane gas pressure that defines both the systematic and anomalous thermal regions over which pure methane hydrate dissociates to  $\text{CH}_4$  gas +  $\text{H}_2\text{O}$  ice or water. The region of anomalous preservation can be easily accessed by the pressure-release treatment at temperatures just below the ice point; successful exploitation of this behavior may thus provide novel application for retrieval of naturally occurring gas hydrate, or for temporary low-pressure transport and storage of manufactured or collected gas hydrate. It is also an effect that has not previously been considered for stability issues involving deep-water drilling into or through hydrate-bearing sediments, or models of seafloor stability where rapid pressure release along fault vents may occur.<sup>30</sup> Furthermore, as only modest additional heating of the preserved material through 273 K is required to initiate release and capture of most of the hydrate-forming gas in a controllable manner, this method may offer additional strategies for controlling gas yield rates from hydrate-bearing deposits.

**Acknowledgment.** We thank Drs. Timothy Collett and Rob Kayen (both USGS) and three anonymous reviewers for providing helpful reviews of the manuscript, and John Pinkston for his technical support. This work was supported in part under the auspices of the USGS and in part by the U.S. DOE by the Lawrence Livermore National Laboratory under Contract W-7405-ENG-48.

## References and Notes

- (1) Kvenvolden, K. *Rev. Geophys.* **1993**, *31*, 173.
- (2) Sloan, E. *Clathrate Hydrates of Natural Gases*, 2nd ed; Marcel Dekker: New York, 1998.
- (3) Lunine, J.; Stevenson, D. *Astrophys. J. Suppl.* **1985**, *58*, 493.
- (4) Borg, I.; Stephens, D.; Bedford, R.; Hill, R. Evaluation of research opportunities in gas hydrates, Lawrence Livermore National Laboratory Report UCID-19755, 1983.
- (5) Kvenvolden, K. *Global Biogeochem. Cycles* **1988**, *2*, 221.
- (6) Kvenvolden, K. *Proc. Natl. Acad. Sci. U.S.A.* **1999**, *96*, 3420.
- (7) Paull, C.; Buelow, W.; Ussler, W.; Boroski, W. *Geology* **1996**, *24*, 143.
- (8) Kayen, R.; Lee, H. *Mar. Geotech.* **1991**, *10*, 125.
- (9) Kennett, K.; Cannariato, K.; Hendy, I.; Behl, R. *Science* **2000**, *288*, 128.
- (10) Stern, L.; Kirby, S.; Durham, W. *Science* **1996**, *273*, 1843.
- (11) Stern, L.; Kirby, S.; Durham, W. *Energy Fuels* **1998**, *12*, 201.
- (12) Stern, L.; Hogenboom, D.; Durham, W.; Kirby, S.; Chou, I.-M. *J. Phys. Chem. B* **1998**, *102*, 2627.
- (13) Five samples synthesized by the methods described previously<sup>10,11</sup> were then dissociated in situ by temperature-ramping procedures (Figure 1B) specifically for determination of compositional reproducibility. One sample also underwent a uniaxial compaction procedure following synthesis to eliminate porosity. All five samples yielded a stoichiometry of  $\text{CH}_4 \cdot n\text{H}_2\text{O}$ , where  $n = 5.89 \pm 0.01$ . This composition is slightly closer to ideal than that which we reported previously ( $6.1 \pm 0.1$ , on samples that contained 0–3% unreacted ice; see refs 10 and 11), due to significantly improved analytical and measurement capabilities provided by our gas flow meter and collection apparatus (see ref 14) and by the internal (sample) thermocouples that now allow detection of very small amounts of unreacted ice. Samples are also now routinely held at the highest  $P$ – $T$  conditions during synthesis for several hours longer than in previous syntheses, to ensure reaction of the last several percent of ice to hydrate. (The difference between  $n$  of 5.89 vs 6.1 in our samples corresponds to 3.2 vol % unreacted

ice.) X-ray diffraction analyses of as-grown material, and reflection microscopy of sample surface replicas indicated a lack of any preferred grain orientation or grain size heterogeneity in the final as-synthesized product (see refs 10 and 11).

(14) The flow meter and gas collection apparatus consists of a hollow, closed-ended stainless steel cylinder that is inverted in a reservoir of distilled water and suspended from a precision load cell (see Figure 1 in ref 15). A column of water is initially drawn up by vacuum into the cylinder, and maintenance of a constant drip of water into and out of the reservoir in which the cylinder is suspended ensures a constant buoyancy force on the cylinder. The reservoir water is saturated with methane prior to dissociation, minimizing further methane solution during testing. The apparatus is plumbed directly in line with the synthesis apparatus, such that opening the sample valve allows gas to flow from the sample to the collection apparatus. As methane gas evolves from the dissociating sample, it enters the inverted cylinder and displaces the water column, thereby decreasing the cylinder weight. The mass of methane collected in the cylinder is then calculated from that weight change, taking into account the temperature inside the cylinder, room pressure, the partial pressure of water vapor in methane, and the equation of state of methane gas. The cylinder volume is 8 L, and a typical 30 g sample of methane hydrate releases close to 6 L of gas during dissociation. The flow meter operates at least over the range 0.07–3000  $\text{cm}^3/\text{min}$  with resolution to 0.01  $\text{cm}^3/\text{min}$  at the slowest rates, and gas mass measurements reported here are accurate to better than 1%.

(15) Circone, S.; Stern, L.; Kirby, S.; Pinkston, J.; Durham, W. In *Gas Hydrates: Challenges for the Future*; Holder, G., Bishnoi, P., Eds.; 2000; pp 544–556.

(16) In early tests, release of trapped pore gas was occasionally detected by the flow meter during the isothermal hold at 190 K and 0.1 MPa prior to heating the sample for dissociation. This release was measured as small but discrete decreases in the load cell weight, usually accompanied by audible crackling of the sample within the pressure vessel. The presence of trapped gas within closed-off pores prior to stoichiometry measurement was eliminated from later experiments by either performing the initial depressurization step at a faster rate (Figure 1B, points 2–3), or by significantly reducing the compaction of the seed ice during sample preparation procedures to produce a more porous final product. Likewise, no evidence was observed to indicate that any measurable adsorbed methane on the surface of the hydrate grains interfered with the stoichiometry measurements and calculations; such methane should desorb during the low-pressure isothermal hold prior to measurement, and no indication of such methane was detected by the flow meter as a baseline drift.

(17) The specific time interval of the rapid pressure release is varied with the magnitude of the initial pressure overstep of the equilibrium curve (see Figure 1B); smaller oversteps require more rapid pressure release, but venting in less than 5 s was found to be less optimal for successful preservation.

(18) Typically,  $100 \pm 3\%$  of the expected total gas yield (based on stoichiometry number  $n = 5.89$ ) was collected by the finish of each rapid-depressurization test after heating through 273 K. In several instances the error margin increased to  $\pm 5\%$ , due to excessive loss of some hydrate-forming gas during the initial venting procedure (resulting in a low yield), or due to small amounts of trapped pore gas being included in the measurement (giving a high yield). The general topology of the flow curves usually made it apparent when the latter was the case, as release of trapped gas typically evolves in pulses, rather than continuous flow.

(19) One sample that was rapidly depressurized at 269 K, “preserved” for 90 min after losing only 8 vol % gas, and then quenched in liquid N, was X-rayed for confirmation of hydrate structure and composition. This sample showed that the sample interior was almost pure sl methane hydrate with  $\leq 5$  vol %  $\text{H}_2\text{O}$  ice, indicating that (1) preserved material was not a new phase that is greatly dissimilar from sl hydrate, (2) the ice product formed during the early dissociation event does not occur homogeneously throughout the sample (on a grain-by-grain basis), but rather on a sample-wide scale, probably initiating at the vented end of the sample, and (3) that no other crystalline or amorphous phases were present at a level exceeding a few volume percent.

(20) Buffett and Zatssepina (Buffett, B.; Zatssepina, O. *Geophys. Res. Lett.* 1999, *26*, 2981), for instance, suggest that gas hydrate in marine environments may persist metastably to several degrees above its nominal equilibrium  $P$ – $T$  stability field, due to maintenance of a high fugacity of the hydrate-forming gas in the surrounding liquid phase. In their model, the barrier to complete dissociation is largely dependent on the free energy requirements for nucleation of small bubbles in such a supersaturated solution, to create a vapor phase.

(21) These pressure-release tests were conducted on pure methane hydrate samples that contained 40–45% pore volume (compared to 29% of standard samples), and on methane hydrate + quartz sand aggregates that were synthesized either as discrete, alternating layers of hydrate or sand, or mixed homogeneously. These samples were all tested at  $268.5 \pm 1.5$  K, but displayed dissociation behavior very similar to those tests shown in Figure 4 between 255–265 K.



- (22) Yakushev, V.; Istomin, V. In *Physics and Chemistry of Ice*; Maeno, N., Hondoh, T., Eds.; Hokkaido University Press: Sapporo, Japan, 1992; pp 136–139.
- (23) Handa, Y.; Stupin, D. *J. Phys. Chem.* **1992**, *96*, 8599.
- (24) Peters, D.; Selim, M.; Sloan, E. In *Gas Hydrates; Challenges for the Future*; Holder, G., Bishnoi, P., Eds.; pp 304–313.
- (25) Davidson, D.; Garg, S.; Gough, S.; Handa, Y.; Ratcliffe, C.; Ripmeester, J.; Tse, J. *Geochim. Cosmochim. Acta* **1986**, *50*, 619.
- (26) Handa, Y. *J. Chem. Thermodyn.* **1986**, *18*, 891.
- (27) Gudmundsson, J.; Parlaktuna, M.; Khokhar, A. *SPE Prod. Facilities* **1994**, *69*.
- (28) Dallimore, S.; Collett, T. *Geology* **1995**, *23*, 527.
- (29) Dash, J.; Fu, H.; Wettlaufer, W. *Rep. Prog. Phys.* **1995**, *58*, 115.
- (30) Other implications of gas hydrate occurrences and partial decomposition, however, have been discussed in the context of such stability issues as increased frequency of slumping and slope failure during the last glacial maximum, when stabilizing influences of pressure were at a minimum (see for example Paull et al.<sup>7</sup> and Kayen and Lee<sup>8</sup>). Buffet and Zatsepina<sup>20</sup> further suggest that gas hydrate metastability may be implicated in such issues, due to sudden decomposition of the metastable material producing substantial pore pressure in the sediments. We note, however, that the mechanism and geochemical requirement for metastability discussed by Buffett and Zatsepina is markedly different from the anomalous preservation effect discussed here.